



Conversion of Green Silica from Corn Leaf into Zeolites Na A-X

Teguh Kurniawan^{1,*}, Dhimas Satria¹, Juniafit Bima Saputra¹, Muhammad Roil Bilad², Nik Abdul Hadi Md Nordin³, Hairus Abdullah⁴

¹Universitas Sultan Ageng Tirtayasa, Cilegon 42435, Indonesia

²Faculty of Integrated Technologies, Universiti Brunei Darussalam, Jalan Tungku Link, Gadong BE1410, Brunei Darussalam

³Department of Chemical Engineering, Universiti Teknologi PETRONAS (UTP), 32610 Seri Iskandar, Malaysia

⁴Department of Industrial Engineering, Universitas Prima Indonesia, Medan, Sumatera Utara, Indonesia

Correspondence: E-mail: teguh@untirta.ac.id

ABSTRACTS

Combustion of corn leaf as a model of biomass from agricultural waste is a simple way to obtain the energy. It produces a low-value by-product of ash and is rich in silica that can become a precursor for zeolite production. In this study, acid-treated corn leaves combustion was performed to produce high purity silica (SiO₂). The diffraction pattern suggested that the extracted silica was amorphous without the impurities phase. Additionally, the nitrogen isotherm indicated that the material was highly mesoporous silica with a total surface area of 200 m²/g. The hydrothermal method was then applied with a composition molar ratio of 1.25SiO₂:1Al₂O₃:5Na₂O:250H₂O to synthesize zeolites from the silica. The temperature and time effect on the hydrothermal zeolite's synthesis was investigated. The diffraction pattern shows that high crystalline zeolite Na A-X was produced at temperatures of 100°C and 8 h hydrothermal time. According to nitrogen physisorption analysis, the zeolite Na A-X consisted of micropores with a total surface area of 270 m²/g. The morphology of zeolite Na A-X was cube for the Na-A and octahedral for the Na-X. The hydrothermal temperature and time highly affected the zeolite formed. This research suggested that the ash waste could be valorized through conversion into a high economic value zeolites.

© 2022 Tim Pengembang Jurnal UPI

ARTICLE INFO

Article History:

Submitted/Received 17 Mar 2022

First revised 23 Apr 2022

Accepted 07 May 2022

First available online 09 May 2022

Publication date 01 Sep 2022

Keyword:

Corn leaf,

Green silica,

Hydrothermal,

Zeolite Na A-X.

1. INTRODUCTION

Indonesia is a largely agricultural country in Southeast Asia. Biomass from agriculture waste is generated in a huge quantity which is a potential renewable source for replacing fossil fuels. Corn is one of the important agricultural commodities in Indonesia. In 2015, corn production reached 19.61 tons, which is also generated by-products of biomass such as the leaves, stalks, and cobs known as corn stover during harvesting. The heating value was 2.64 MJ/kg of air and fuel mixture for dried corn stover (Wang *et al.*, 2011). The corn stover combustion process, however, generated ash which would become waste and an environmental problem.

Zeolite is microporous crystalline material of aluminosilicates with 3- dimensional framework structures composed of corner-sharing TO₄ tetrahedra (T is Si or Al). Cations at the extra-framework position compensate for the negative charge due to the presence of alumina tetrahedra. Silica is required for synthesizing zeolite, which is commercially available from non-renewable sources. Silica reported could be extracted from various biomass such as rice husk, bamboo leaves, grass corn cob (Olawale, 2020; Pięła *et al.*, 2020; Shim *et al.*, 2015; Steven *et al.*, 2021).

Among other parts of corn, the ash of corn leaf is the richest in silica (Lanning *et al.*, 1980), which may potentially be applied as a precursor to synthesize zeolites. Leaves are the second-highest (22%-wt.) component after stalks (50%-wt.) on the corn stover (Morissette *et al.*, 2011). Leaves contain the highest ash content among other corn stover components with 10.4% (Lacey *et al.*, 2016). In addition, the silica content in corn leaf is 7 times higher than the stalk fraction (Li *et al.*, 2012).

The high ash content of corn leaves potential to obtain a high yield of green silica. Acid treatment was needed to improve the purity and surface area (Shakouri *et al.*, 2020; Steven *et al.*, 2021). Silica is a precursor in

zeolite synthesis. Hence, the silica obtained from corn leaves could replace the non-renewable silica used at present time.

There are groups reported that ash derived from various biomass such as rice husk, bamboo leaves, common water reeds, and corn stover could be converted into various types of zeolites (Al-Jubouri *et al.*, 2021; Ng *et al.*, 2017; Pangan *et al.*, 2016, 2021; Simanjuntak *et al.*, 2021). Zeolite Na-A was obtained from corn stover ash (Pangan *et al.*, 2021).

The ash corn stover showed a crystalline phase detected by diffraction patterns such as calcite, cristobalite, and quartz. The calcination and acid treatment of corn stover ash cannot destroy the aggregation crystal phase. The combustion temperature significantly drives the formation of the crystal phase of silica which at a temperature of more than 700°C favored the formation of crystalline silica (Steven *et al.*, 2021).

The investigation aimed to synthesize zeolite Na-AX from corn leaf by hydrothermal method. The corn leaf was prepared by acid treatment and combustion at low temperatures to obtain highly amorphous silica. The effect of temperature and time of hydrothermal synthesis was also studied. To the best of our knowledge, the research is the origin and could enhance our understanding of the synthesis of zeolite from green silica of biomass.

2. METHODS

In this section, an experimental method that consists of silica extraction, hydrothermal synthesis, and material characterization is explained. The silica extraction and hydrothermal synthesis steps are performed in the Faculty of Engineering, Universitas Sultan Ageng Tirtayasa. The characterization material was performed in Universiti Teknologi PETRONAS (UTP).

2.1. Silica Extraction

Corn leaves were obtained from Natar, Lampung Province, Indonesia. The corn variety was Hybrid NK-22 which was planted during the dry season. Before use, corn leaves were washed with distilled water to remove dust and dried in the sun. The dried corn leaves were cut 3 cm in length, weighed 45 g, and treated with 1 L of 1.5 M HNO₃ (Merck) using a mixer agitator at 90 rpm for 15 h at room temperature. The acid-treated corn leaves were filtered and washed with distilled water to pH 7. After that, the corn leaves were mashed with a blender. Furthermore, the corn leaves were burnt in the furnace at a temperature of 600°C for 6 h. The green silica obtained was 3 g with a yield of 6.67%.

2.2 Hydrothermal Synthesis

The synthetic zeolite was prepared by hydrothermal method with a molar ratio of 1.25SiO₂: 1Al₂O₃: 5Na₂O: 250H₂O. **Table 1** present the experiment to study the effect of time and temperature. The hydrothermal method was adapted from literature (Ng *et al.*, 2017). Here we explain samples A-4 for the detailed hydrothermal procedure. First, an amount of 4.16 g of NaOH (Merck) was dissolved in 18.94 mL of distilled water, then 2.55 g of sodium aluminate (Sigma Aldrich) was added and stirred at room temperature until homogenous. After that, 1.05 g of silica was added to 44.21 mL of distilled water in a separate place.

The aluminate solution was added to the silicate solution and stirred at 600 rpm using a magnetic stirrer for 10 min. After that, the solution was poured into a Polytetrafluoroethylene (PTFE)-coated autoclave to perform the hydrothermal process. The autoclave was put into the oven for 8 h at 100°C. The hydrothermal precipitate was washed using distilled water several times until it reached a neutral pH and allowed to stand at room temperature for 24 h. After that, the sample was dried in the oven for 6 h at a temperature of 110°C.

2.3 Material Characterization

Characterization of samples was carried out by several analyses, i.e., an X-ray diffraction (XRD), a Scanning Electron Microscopy (SEM), a Nitrogen Physisorption, an X-Ray Fluorescence (XRF), and a Fourier-Transform Infrared Spectroscopy (FTIR). A Rigaku Miniflex 600 type was used for XRD analysis by using a measurement angle of 2θ 5-50° with step size 0.01° to identify the crystal phase structure. SEM analysis was performed to study the morphology of the sample using CAL M2566 21 08 type Normi. Nitrogen Physisorption was performed to study textural properties by using TriStar II Plus Version 3.02. The Bruker Vertex80v Beam was used for the FTIR study. The samples were mixed with KBr and pelletized followed by analysis with resolution 2 cm⁻¹ and transmittance scan number 200.

Table 1. Temperature and time effect experiment via hydrothermal zeolite synthesis.

Effect of Parameters	Samples	Temperature (°C)	Time (h)
Time	A-1	100	2
	A-2		4
	A-3		6
	A-4		8
Temperature	A-5	75	8
	A-6	85	
	A-7	95	
	A-8	100	

3. RESULTS AND DISCUSSION

3.1. Silica Extracted from Corn Leaves

Figure 1 presents the XRD pattern of corn leaf ash acid-treated. The silica diffractogram pattern shows a hump between $2\theta = 15 - 30^\circ$ which indicated that the silica of corn leaf ash has an amorphous phase. There are no sharp peaks on the diffraction pattern which suggested that the crystalline silica was not formed. Low combustion temperature (below 700°C) within a short time process favored the formation of amorphous silica (Chen *et al.*, 2015). The silica in the amorphous phase has a random and irregular arrangement of atoms and patterns so that amorphous silica is more reactive than crystalline silica (Kirk *et al.*, 1953). The non-zeolite crystalline phases i.e., CaCO_3 and SiO_2 silicate reduced in the acid treatment method as reported elsewhere (Pangan *et al.*, 2016; Steven *et al.*, 2021; Suwanmaneechot *et al.*, 2015; Wu *et al.*, 2018). Nitric acid as a strong acid successfully removed the metals by extracting them into the acid solution. Therefore, silica from corn

leaf ash was pure and can be used as a source of silica for zeolite synthesis.

3.2. Effect of Hydrothermal Time on Zeolite Crystallinity

Figure 2 presents the XRD results of zeolite synthesis from corn leaf ash with variations in hydrothermal processing time. After 2 h hydrothermal time, Na-A phase zeolite was formed which had a high purity of nearly 100%, however, the peak intensity of the resulting Na-A phase zeolite was relatively low. The longer hydrothermal time, i.e., 4, 6, and 8 h, favored the intergrowth crystal phase of Na-A and Na-X. As the hydrothermal time increased, the Na-X zeolite had a higher intensity peak while the Na-A was remaining exist. It can be seen at peaks $2\theta = 6.23, 11.82, 15.52, 23.40, 26.78, 31.68, 37.49,$ and 42.77° which is similar to the standard diffraction pattern of Na-X. At 4 - 8 h, a new phase of zeolite was seen, namely Sodalite at peaks of $2\theta = 14.07^\circ$ and 14.02° (**Figure 2**). As the hydrothermal time is longer, Na-X phase zeolite has a higher intensity peak.

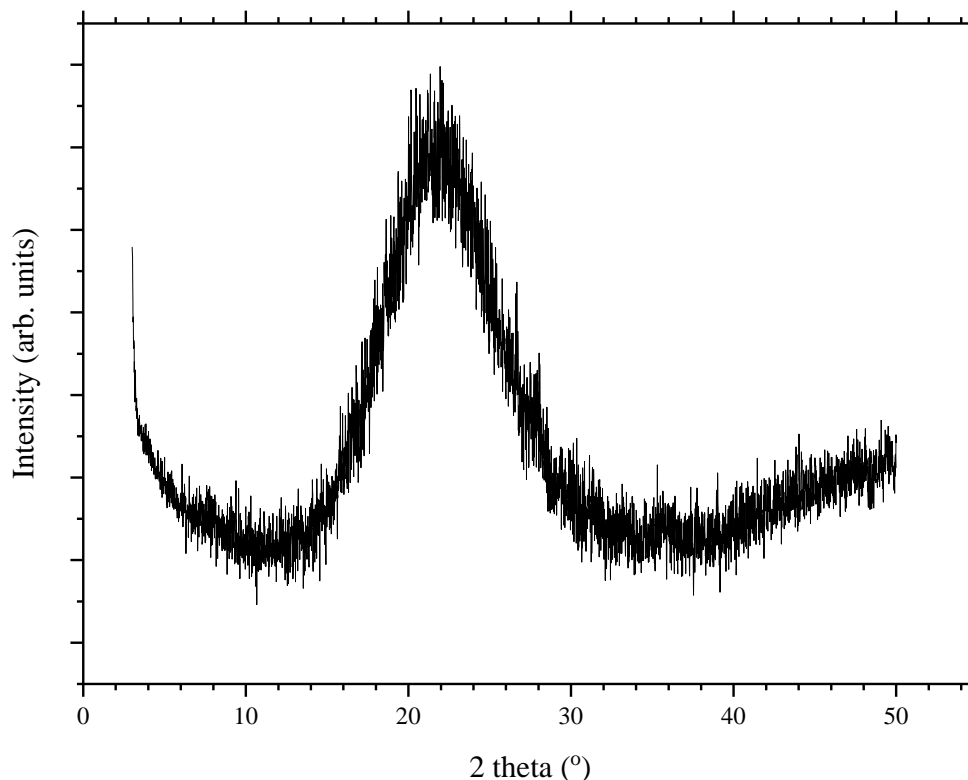


Figure 1. XRD Analysis on Silica from Corn Leaves.

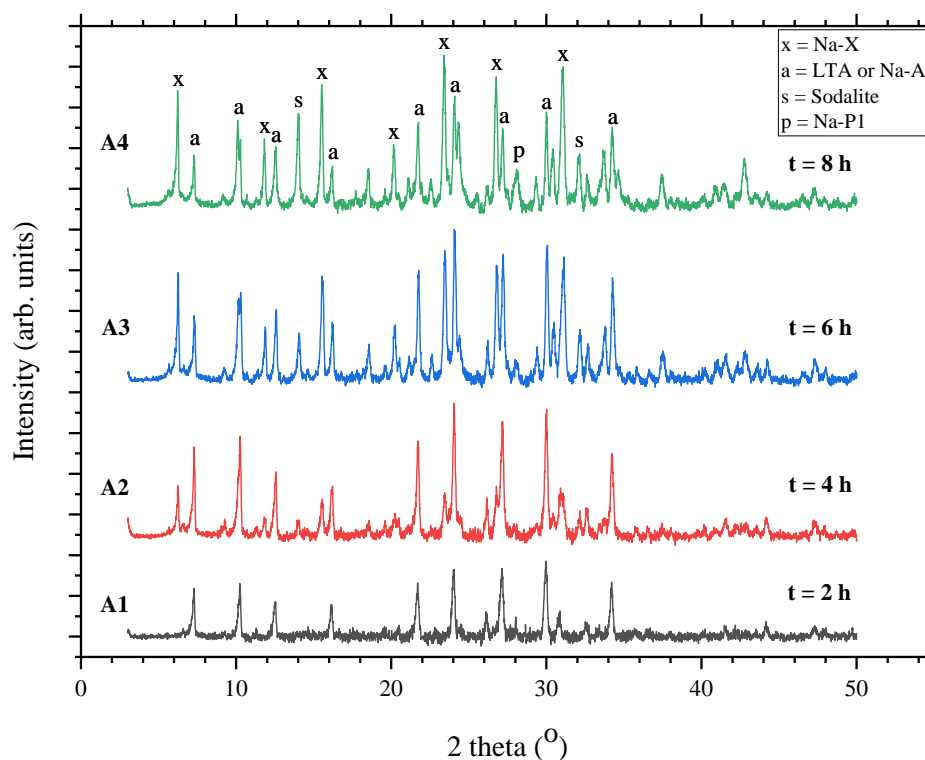


Figure 2. XRD pattern of the synthetic zeolites with a hydrothermal time of 2, 4, 6, and 8 h at a temperature of 100°C.

Therefore, the crystallization time affects significantly the formation of Na A-X zeolites. This is in agreement with literature reported elsewhere (Yao *et al.*, 2018). Apart from the different times, the zeolite Na A-X peaks can be seen clearly in all the products, and the crystallinity of the products increases and then decreases with the extension of the hydrothermal time. According to Wu *et al.* (2018), zeolite Na A-X derived from coal fly ash showed the highest crystallinity when the hydrothermal time was at a temperature of 100°C for 6 h. This is in agreement with our results that the crystallinity of intergrowth zeolite Na A-X was high at 6-8 h.

3.3. Effect of Hydrothermal Temperature on Zeolite Crystallinity

The temperature effect on diffraction patterns is presented in Figure 3. The results obtained according to XRD analysis at a temperature of 75, 85, and 95°C were a mixture of Na-A and Na-X phase zeolite. However, when the crystallization

temperature increased to 100 °C, a mixture of Na-A, Na-X, and Sodalite phase zeolite was found at peak $2\theta = 14.02^\circ$ as marked in Figure 3. At temperatures of 75, 85, and 95 °C, the Na-A and Na-X zeolite peaks increased simultaneously. At a temperature of 100°C, the Na-X phase increased, while the Na-A phase decreased and a new zeolite sodalite phase appeared.

Yao *et al.* (2018) investigated the synthesis of zeolite X from natural low-grade diatomite as a silica source. Silica from diatomite did not react with $\text{Al}(\text{OH})_3$ at 90 °C in an alkaline solution. When the temperature increased by 100 °C, zeolite X started to crystallize. Then, when the temperature was 110 °C zeolite X, a pure crystalline single phase is formed. When the temperature is raised to 120 °C, zeolite X is formed with some impurity of zeolite A appeared.

Therefore it should be noted that increasing temperature will accelerate crystal nucleation and growth of zeolite A and X (X. Liu & Wang, 2017).

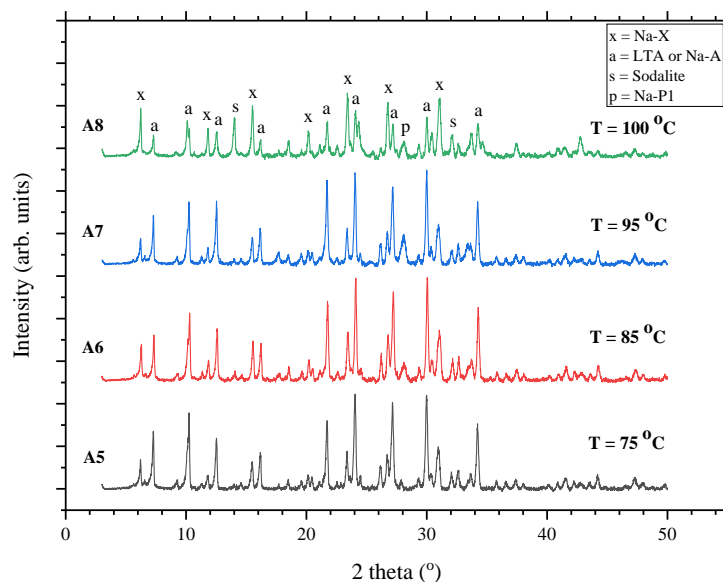


Figure 3. XRD analysis on synthetic zeolite with a hydrothermal temperature of 75, 85, 95, and 100°C at a time of 8 h.

3.4. Morphology of corn leaf ash silica

The morphologies of silica from corn leaves samples were examined and the corresponding SEM micrographs are shown in **Figure 4**. The extracted corn leaf silica was carried out at a magnification of 100 - 5000 times. The morphology of corn leaf ash on the surface appears random and not smooth. These results are consistent with the XRD

analysis that has been carried out that the product formed was non-crystalline. The observations made by analyzing SEM results using silica samples from sand sources also have non-uniform particle sizes and tend to clump (Silahooy, 2020). In addition, rice husk silica extracted by SEM analysis was also reported as an irregular morphology (Purwaningsih *et al.*, 2018).

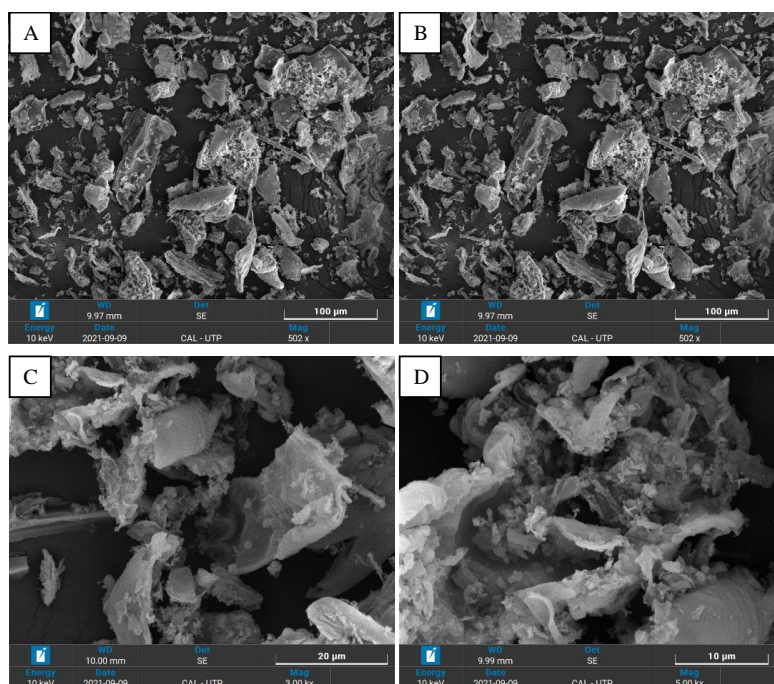


Figure 4. SEM images on Silica from corn leaves. (a) 500x magnification, (b) 1000x magnification, (c) 3000x magnification, (d) 5000x magnification.

3.5. Effect of Hydrothermal Time on the Morphology of Synthetic Zeolite

The morphology of the synthesized Na-AX samples was examined, and the corresponding SEM micrographs are shown in **Figure 5**. The results of SEM at a hydrothermal time for 2 h formed a solid cube crystal of zeolite A without other zeolite impurities, however some amorphous are still visible as pointed by the arrow. The morphology of Na-A crystals as the cube is similar to the work reported in the literature (Liu *et al.*, 2013; Ng *et al.*, 2017). At 4 h of hydrothermal, octahedral crystals begin to appear which are the Na-X zeolite morphology. This is consistent with the reference results of Na-X crystal morphology studied by other groups (García, 2016; Lee *et al.*, 2007; Zhang *et al.*, 2019). Zeolite Na-A has higher crystallinity than Na-X zeolites. Zeolite sodalite impurity appeared as a ball morphology. This result is consistent with the work of (Hums, 2017). In Aminatus's work, he reported that at 4 h hydrothermal, the morphology of zeolite cubes Na-A is not

uniform because it contains impurities in the form of sodalites with spherical morphology. At a longer hydrothermal time of 6 to 8 h zeolite Na-AX has almost the same high intensity, this can be seen in the results of the morphological analysis which showed zeolite A and X increasingly robust and clear in shape. At this time, sodalite impurities zeolite also increase and in line with the emergence of pseudo-spherical morphology i.e. Na-P crystals. Research conducted by Liu explained the discovery of pseudo-spherical or sodalite morphology at a hydrothermal time for 8 h (Liu *et al.*, 2013). The average crystal size was as expected, the visible cube-shaped Na-A zeolite had an average diameter of 1.89 μm , while the octahedral Na-X zeolite had an average diameter of 3.58 μm . Based on the above SEM morphological analysis, these results are consistent with the XRD analysis in **Figure 2**, which shows that a longer hydrothermal time resulted in an increase in the crystallinity intensity of higher Na-AX zeolite and produce pure Na-AX zeolite phase, i.e. at hydrothermal time of 6 and 8 h.

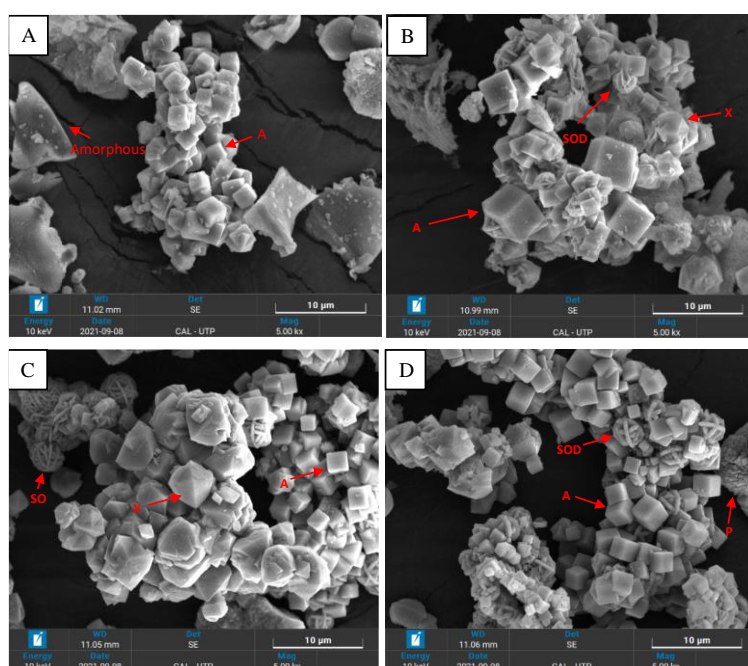


Figure 5. SEM images of the Na-AX at different hydrothermal reaction times. (a) 2 h, (b) 4 h, (c) 6 h, and (d) 8 h.

3.6. Effect of Hydrothermal Temperature on the Morphology of Synthetic Zeolites

Figure 6 presents the SEM images of various hydrothermal temperatures. The SEM micrograph at a hydrothermal temperature of 75°C showed a cube morphology which indicated the Na-A zeolite. The octahedral morphology also appeared which suggested the Na-X zeolites. At this temperature, the visible impurities are in the form of feather ball-like and false ball-like morphology namely sodalite zeolite and Na-P zeolite with low intensity. Furthermore, at higher temperatures of 85 – 95°C the morphology of Na-A zeolite and Na-X zeolite has the same intensity as the lower temperature, but the morphology is more visible and sharp. At higher temperatures, the impurities of sodalite zeolite and Na-P zeolite increased, this can be seen from the morphology of the ball yarn and the false ball which looks perfect and increased in number. Furthermore, at a hydrothermal temperature of 100 °C, cube and octahedral morphologies are visible which are characteristic of very clear and sharp Na-AX

zeolites with almost identical intensities. The average crystal size was as expected, the visible cube-shaped Na-A zeolite had an average diameter of 1.74 μm, while the octahedral Na-X zeolite had an average diameter of 2.93 μm. This is in line with the study of Ng et al. (2017) which explained that at a hydrothermal temperature of 70 - 100°C dominant zeolite type was Na-A with cube morphology. At a temperature of 100°C sodalite zeolite impurities grow between the crystal cubes as also reported elsewhere (Ng et al., 2017). In another study also described, at hydrothermal temperatures of 90 °C and 100 °C octahedral or rhombus-like morphology appeared on the surface of the material. Furthermore, at higher temperatures, zeolite sodalite impurities begin to grow whose morphology is like a ball. Based on the above SEM characterization results, these results are consistent with the XRD analysis in Figure 3 which explains that the higher the hydrothermal temperature used, the higher the crystallinity of the Na-AX and the impurities.

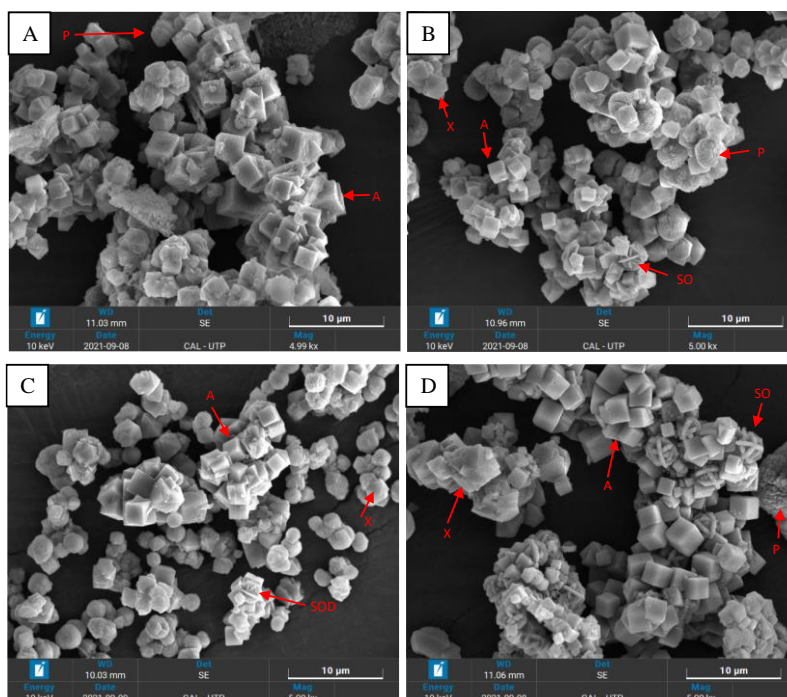


Figure 6. SEM images of the Na-AX at different hydrothermal reaction temperature. (a) 75 °C, (b) 85 °C, (c) 95 °C, and (d) 100 °C.

3.6. Textural Properties of Corn Leaf Ash Silica

Based on **Figure 7**, the corn leaf ash silica formed is type IV based on IUPAC classification for adsorption-desorption isotherm and wide hysteresis loop at a relative pressure (P/P_0) 0.4–1.0 indicating the presence of mesoporous (Thommes *et al.*, 2015). This hysteresis loop can also be concluded that silica has plate-like particle aggregates to have pores (Sangwichien *et al.*, 2002). The results of surface area analysis and pore volume characteristics in other studies with silica sources are presented in **Table 2**. Other silica sources used in the form of corn leaf ash have a high surface area of

199.34 m^2/g with an average particle size of 7.03 nm in corn leaf silica, then rice husk has a surface area of 196.66 m^2/g compared to sugarcane ash and corn cobs 80.10 m^2/g and 115.24 m^2/g . Compared to other silica sources, corn leaf silica ash has the largest surface area. Thus, corn leaf ash has the potential for greater adsorption capacity (Setiawan *et al.*, 2020; Yu *et al.*, 2020; Zulkifli *et al.*, 2013). The surface area of a zeolite is influenced by the particle/pore size, pore shape, and pore arrangement in the particle. The pore diameter of various silica sources is quite large, based on IUPAC it can be classified as a mesoporous material as the pore size ranges between 2-50 nm (Kalapathy *et al.*, 2000; Liou & Yang, 2011).

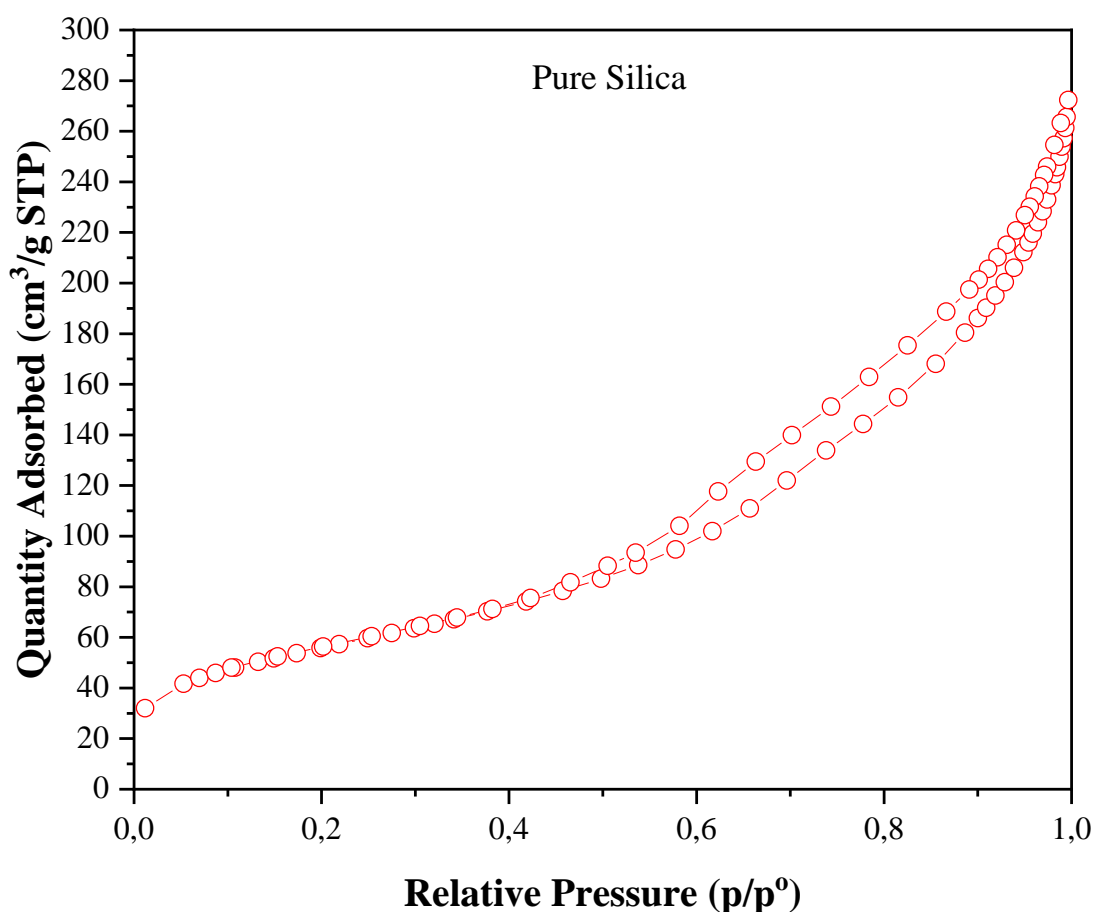


Figure 7. N₂ Adsorption-Desorption Isotherm on Corn Leaf Ash Silica.

Table 2. BET surface area, pore volume, pore diameter, and particle size on silica sources from various studies.

Sample	BET surface area (m ² g ⁻¹)	Pore volume (cm ³ g ⁻¹)	Average pore diameter (nm)	Average particle size (nm)	Particle size range (nm)	Reference
Corn Leaf	200	0.35	7.03	7.84	1.83-169.31	This Works
Rice Husk	197	0.24	4.89	226.37	78-435	(Zulkifli <i>et al.</i> , 2013)
Sugar Cane Ash	80	2.26	112.71	-	-	(Setiawan <i>et al.</i> , 2020)
Corn cob	115	0.11	3.81	-	-	(Yu <i>et al.</i> , 2020)

3.7. Effect of Hydrothermal Time on the Surface Area Analysis of Synthetic Zeolite

Figure 8 shows the adsorption isotherm of the zeolite at different hydrothermal times. It can be seen from the figure that the isotherms are type I which suggested that the materials are highly microporous. At 2 h hydrothermal time, the hysteresis loop is found at a relative pressure (P/P₀) of 0.9-1.0. It is most likely that the amorphous silica contributed to the hysteresis.

The hysteresis has a narrow loop with almost vertical and parallel adsorption and desorption branches (Sangwichien *et al.*, 2002). At this time, the mixture of Na-AX zeolites and amorphous silica has mesoporous. Na-AX zeolite samples at 4–8 h have microporous material characteristics, as they can absorb N₂ gas at low pressure (P/P₀ < 0.3) (Deng *et al.*, 2012).

Furthermore, the results of surface area analysis and pore volume at Na-AX zeolite hydrothermal time variation are shown in Table 3. The longer the hydrothermal process, the larger the BET area and the total volume of Na-AX zeolite. In addition, the

number of micropore volumes is relatively dominant. At 4–8 h hydrothermal time, Na-AX zeolites are dominated by micropores, while at 2 h hydrothermal time still form mesoporous material. This proves that materials treated with hydrothermal treatment with time variation have a large influence on the surface area of Na-AX zeolite.

Another study by Ryu *et al.* (2019) synthesized zeolites from waste from blast furnace combustion with hydrothermal temperature variations of 25, 50, 90, 120, and 150°C. The surface area of BET at a hydrothermal temperature of 50°C decreases compared to a temperature of 25°C, but at a temperature of 90°C the BET model showed a large surface area due to the formation of FAU type zeolite, while at a temperature of 120-150°C, it continues to decrease.

This is due to the change in content between hydroxyapatites, FAU-type zeolites, and hydroxyapatites. The surface area of BET formed was 98.74 m²/g at a hydrothermal temperature of 90 °C (Ryu *et al.*, 2019).

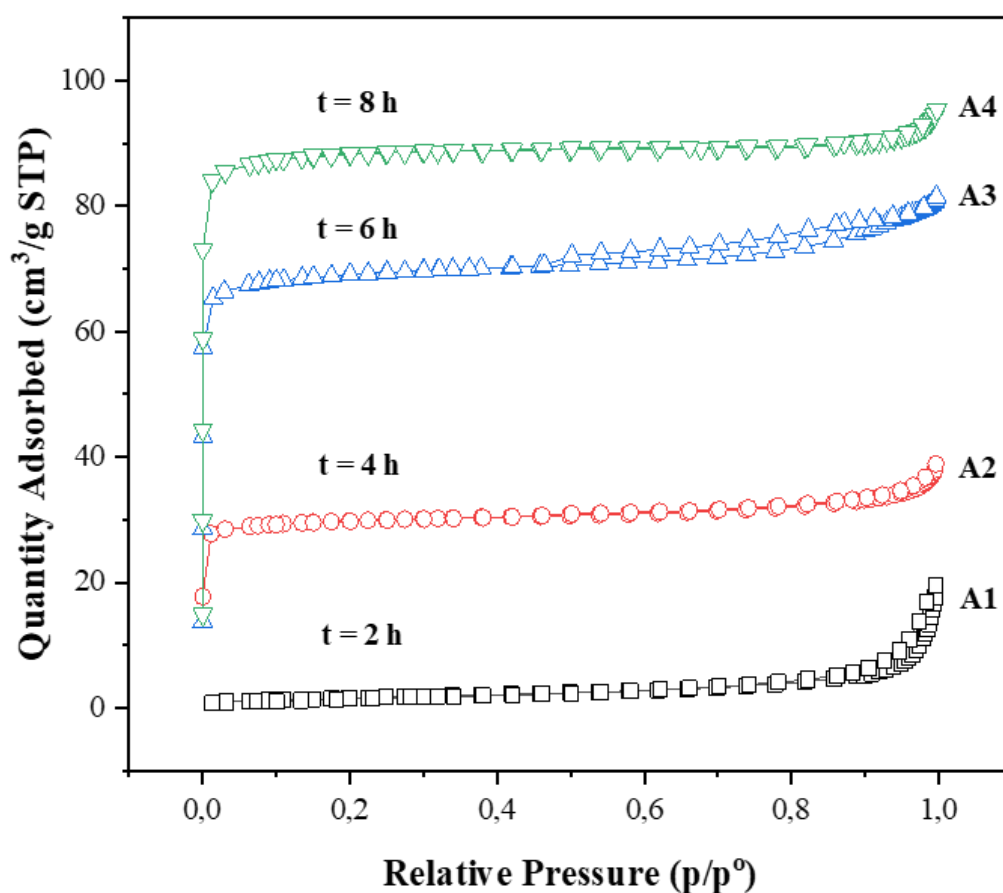


Figure 8. N₂ Adsorption-desorption isotherm of the Na-AX zeolite at different hydrothermal reaction time.

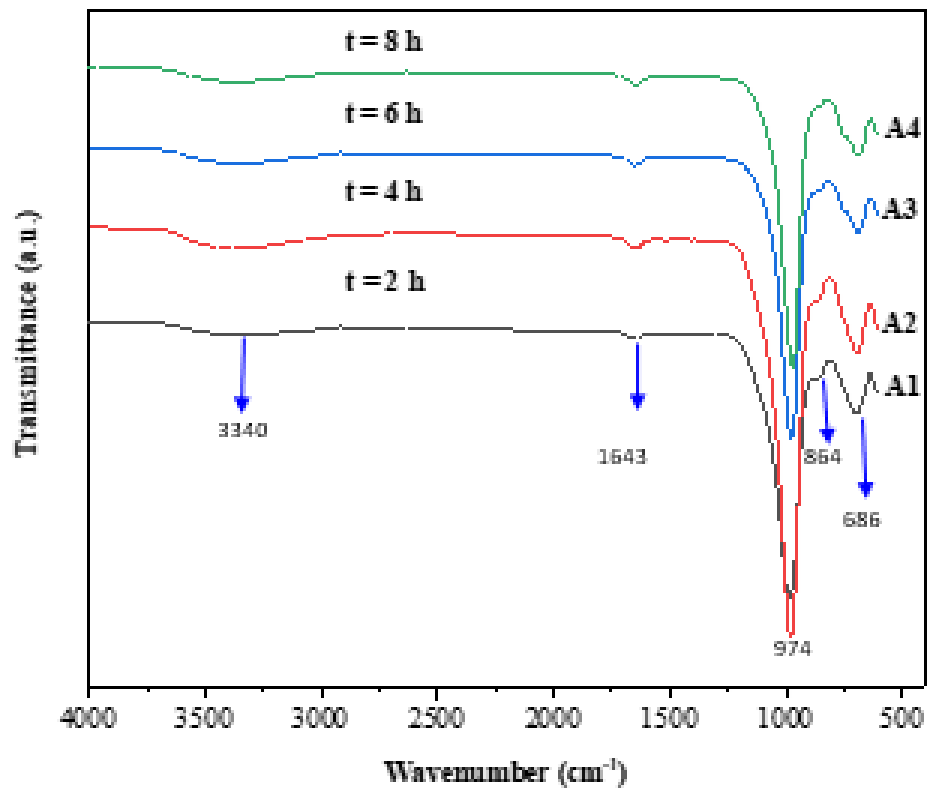
Table 3. Surface area and pore volume on Na-AX zeolite hydrothermal temperature variations.

Sample	BET surface area [m ² g ⁻¹]	Mikropore Area [m ² g ⁻¹]	Mesopore Area [m ² g ⁻¹]	Volume Total [cm ³ g ⁻¹]	Mikropore Volume [cm ³ g ⁻¹]	Mesopore Volume [cm ³ g ⁻¹]
A1-2h	5.89	0	5.89	0.02	0	0.0208
A2-4h	91.80	81.23	10.57	0.05	0.04	0.01
A3-6h	212.19	192.62	19.57	0.12	0.09	0.03
A4-8h	269.87	252.38	17.49	0.14	0.12	0.02

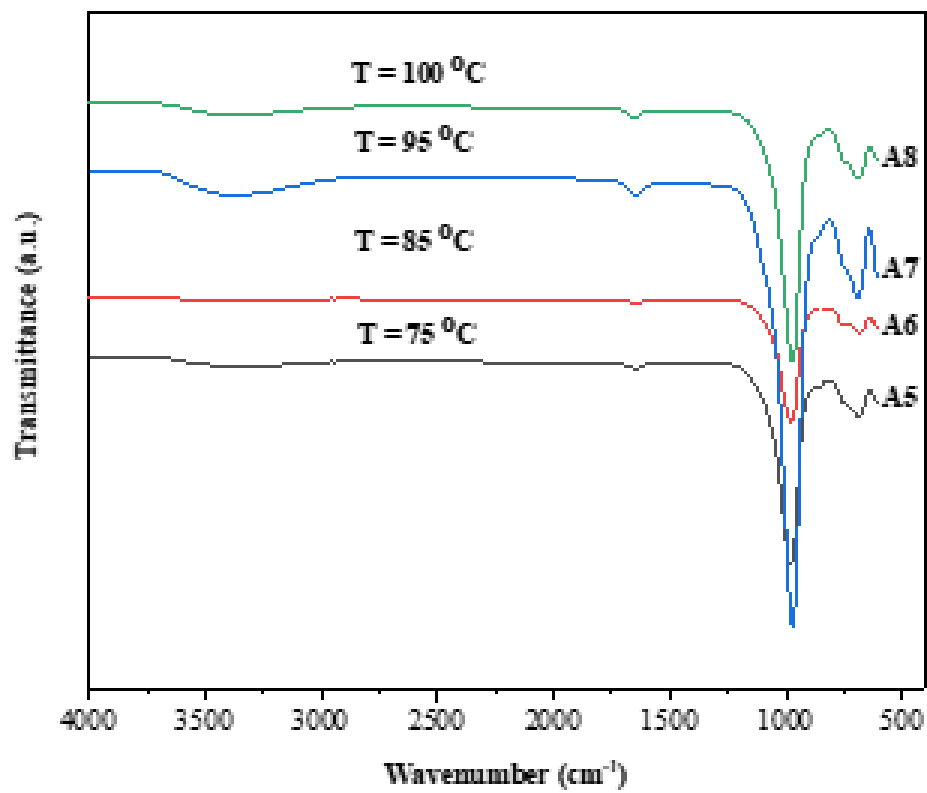
3.9 Effect of Hydrothermal Time and Temperature on the FTIR

Figures 9(a) and (b) present the FTIR Spectra of the Na-AX zeolite at different hydrothermal reaction times and temperatures, respectively. The bands at 3700 - 3400 cm⁻¹ are known to be assignable to Si-OH, Si-OH-Al, and -OH hydroxyl groups, while the bands at about 1560–1690 cm⁻¹ were attributed to the vibration of HOH. The

HOH most likely appeared as water adsorbed in the zeolite's pore. Wavenumbers 989 cm⁻¹ are ascribed to asymmetric stretching vibrations of bridge bonds (*vas* Si-O(Si) and *vas* Si-O(Al)) at wavenumber 741 cm⁻¹ is attributed to the symmetric stretching vibrations of bridge bond (*vs* Si-O-Si). At wavenumber 686 cm⁻¹ is attributed to the symmetric stretching vibrations of bridge bonds– *vs* Si-O-Al (Król *et al.*, 2012; Nandiyanto *et al.*, 2019



(a)



(b)

Figure 9. FTIR Spectra of the Na-AX zeolite at different hydrothermal reactions (a) time and (b) temperature.

4. CONCLUSION

High purity silica has been successfully produced from the combustion of an acid-treated corn leaf. The diffraction pattern suggested that the extracted silica was an amorphous phase with a total surface area of 200 m²/g. Zeolite Na-A-X was successfully produced by hydrothermal method with a molar ratio of 1.25SiO₂:1Al₂O₃:5Na₂O:250H₂O using the silica from corn leaf. Temperature and time effect on the hydrothermal zeolite's synthesis was affected significantly by zeolite phase and crystallinity. The diffraction pattern shows that high crystalline zeolite Na A-X was produced at temperatures of 100°C

and 8 h hydrothermal time. According to nitrogen physisorption analysis, the zeolite Na A-X consisted of micropores with a total surface area of 270 m²/g. The morphology of zeolite Na A-X was a cube for the Na-A and octahedral for the Na-X. In the future, the silica extraction would be beneficial to be performed before combustion to reduce the silica content in the corn leaf, hence the ash problem in the reactor could be avoided.

5. AUTHORS' NOTE

The authors declare that there is no conflict of interest regarding the publication of this article. The authors confirmed that the paper was free of plagiarism.

6. REFERENCES

- Al-Jubouri, S. M., Al-Batty, S. I., and Holmes, S. M. (2021). Using the ash of common water reeds as a silica source for producing high purity ZSM-5 zeolite microspheres. *Microporous and Mesoporous Materials*, 316, 110953.
- Chen, G., Du, G., Ma, W., Yan, B., Wang, Z., and Gao, W. (2015). Production of amorphous rice husk ash in a 500 kW fluidized bed combustor. *Fuel*, 144, 214-221.
- Deng, H., Yi, H., Tang, X., Yu, Q., Ning, P., and Yang, L. (2012). Adsorption equilibrium for sulfur dioxide, nitric oxide, carbon dioxide, nitrogen on 13X and 5A zeolites. *Chemical Engineering Journal*, 188, 77-85.
- García, A., López, C. M., García, L. V., Casanova, J., and Goldwasser, M. R. (2016). Improvements in the synthesis of zeolites with low Si/Al ratio from Venezuelan sodium silicate for an environmentally friendly process. *Ingeniería e Investigación*, 36(1), 62-69.
- Hums, E. (2017). Synthesis of phase-pure zeolite sodalite from clear solution extracted from coal fly ash. *Journal Thermodyn Catal*, 8(02), 1000187.
- Kalapathy, U., Proctor, A., and Shultz, J. (2000). A simple method for production of pure silica from rice hull ash. *Bioresource Technology*, 73(3), 257-262.
- Kirk, R. E., Othmer, D. F., and Newburger, S. H. (1953). Encyclopedia of Chemical Technology. *Journal of Aoac International*, 36(4), 1190a – 1191.
- Król, M., Mozgawa, W., Jastrzębski, W., and Barczyk, K. (2012). Application of IR spectra in the studies of zeolites from D4R and D6R structural groups. *Microporous and Mesoporous Materials*, 156, 181-188.
- Lanning, F. C., Hopkins, T. L., and Loera, J. C. (1980). Silica and ash content and depositional patterns in tissues of mature *Zea mays* L. plants. *Annals of Botany*, 45(5), 549-554.

- Lee, H. J., Kim, Y. M., Kweon, O. S., and Kim, I. J. (2007). Structural and morphological transformation of NaX zeolite crystals at high temperature. *Journal of the European Ceramic Society*, 27(2-3), 561-564.
- Li, Z., Zhai, H., Zhang, Y., and Yu, L. (2012). Cell morphology and chemical characteristics of corn stover fractions. *Industrial Crops and Products*, 37(1), 130-136.
- Liou, T. H., and Yang, C. C. (2011). Synthesis and surface characteristics of nanosilica produced from alkali-extracted rice husk ash. *Materials Science and Engineering: B*, 176(7), 521-529.
- Liu, X. D., Wang, Y. P., Cui, X. M., He, Y., and Mao, J. (2013). Influence of synthesis parameters on NaA zeolite crystals. *Powder Technology*, 243, 184-193.
- Liu, X., and Wang, R. (2017). Effective removal of hydrogen sulfide using 4A molecular sieve zeolite synthesized from attapulgite. *Journal of Hazardous Materials*, 326, 157-164.
- Morissette, R., Savoie, P., and Villeneuve, J. (2011). Combustion of corn stover bales in a small 146-kW boiler. *Energies*, 4(7), 1102-1111.
- Nandiyanto, A. B. D., Oktiani, R., and Ragadhita, R. (2019). How to read and interpret FTIR spectroscopy of organic material. *Indonesian Journal of Science and Technology*, 4(1), 97-118.
- Ng, E. P., Chow, J. H., Mukti, R. R., Muraza, O., Ling, T. C., and Wong, K. L. (2017). Hydrothermal synthesis of zeolite A from bamboo leaf biomass and its catalytic activity in cyanoethylation of methanol under autogenic pressure and air conditions. *Materials Chemistry and Physics*, 201, 78-85.
- Olawale, O. (2020). Bamboo leaves as an alternative source for silica in ceramics using Box Behnken design. *Scientific African*, 8, e00418.
- Pangan, N., Gallardo, S., Gaspillo, P. A., Kurniawan, W., Hinode, H., and Promentilla, M. (2021). Hydrothermal synthesis and characterization of zeolite A from corn (zea mays) stover ash. *Materials*, 14(17), 4915.
- Pangan, N., Gallardo, S., Gaspillo, P. A., Kurniawan, W., Hinode, H., and Promentilla, M. (2021). Hydrothermal synthesis and characterization of zeolite A from corn (zea mays) stover ash. *Materials*, 14(17), 4915.
- Pieła, A., Żymańczyk-Duda, E., Brzezińska-Rodak, M., Duda, M., Grzesiak, J., Saeid, A., and Klimek-Ochab, M. (2020). Biogenic synthesis of silica nanoparticles from corn cobs husks. Dependence of the productivity on the method of raw material processing. *Bioorganic Chemistry*, 99, 103773.
- Purwaningsih, H., Ervianto, Y., Nurdiansyah, H., Rahmawati, Y., and Susanti, D. (2018). Pengaruh Penambahan SiO₂ Hasil Ekstraksi Sekam Padi Pada Sintesis Natrium Superionik Konduktor (NASICON) dan Sifat Konduktivitas Ionik Baterai Elektrolit Padat. *Jurnal Fisika*, 8(2), 68-77.
- Ryu, G. U., Kim, G. M., Khalid, H. R., and Lee, H. K. (2019). The effects of temperature on the hydrothermal synthesis of hydroxyapatite-zeolite using blast furnace slag. *Materials*, 12(13).

- Sangwichien, C., Aranovich, G. L., and Donohue, M. (2002). Density Functional Theory Predictions of Adsorption Isotherms With Hysteresis Loops. *Colloids and Surfaces A: Physicochemical and Engineering Aspects*, 206, 313–320.
- Setiawan, A., Hanun, J. N., and Afiuddin, A. E. (2020). Sintesis dan Karakterisasi Zeolit dari Abu Bagasse Sebagai Adsorben Logam Berat Cu(II). *Jurnal Presipitasi*, 17(1), 85–95.
- Shakouri, M., Exstrom, C. L., Ramanathan, S., Suraneni, P., and Vaux, J. S. (2020). Pretreatment of corn stover ash to improve its effectiveness as a supplementary cementitious material in concrete. *Cement and Concrete Composites*, 112, 103658.
- Shim, J., Velmurugan, P., and Oh, B.-T. (2015). Extraction and physical characterization of amorphous silica made from corn cob ash at variable pH conditions via sol gel processing. *Journal of Industrial and Engineering Chemistry*, 30, 249–253.
- Silahooy, S. (2020). Analisis Serbuk Silika Amorf (SiO₂) Berbahan Dasar Pasir. *Science Map Journal*, 2(2), 75-78.
- Simanjuntak, W., Pandiangan, K. D., Sembiring, Z., Simanjuntak, A., and Hadi, S. (2021). The effect of crystallization time on structure, microstructure, and catalytic activity of zeolite-A synthesized from rice husk silica and food-grade aluminum foil. *Biomass and Bioenergy*, 148, 106050.
- Solar, J., De Marco, I., Caballero, B. M., Lopez-Urionabarrenechea, A., Rodriguez, N., Agirre, I., and Adrados, A. (2016). Influence of temperature and residence time in the pyrolysis of woody biomass waste in a continuous screw reactor. *Biomass and Bioenergy*, 95, 416-423.
- Steven, S., Restiawaty, E., Pasymi, P., and Bindar, Y. (2021). An appropriate acid leaching sequence in rice husk ash extraction to enhance the produced green silica quality for sustainable industrial silica gel purpose. *Journal of the Taiwan Institute of Chemical Engineers*, 122, 51-57.
- Suwanmaneechot, P., Nochaiya, T., and Julphunthong, P. (2015). Improvement, characterization and use of waste corn cob ash in cement-based materials. *IOP Conference Series: Materials Science and Engineering*, 103, 12023.
- Thommes, M., Kaneko, K., Neimark, A. V., Olivier, J. P., Rodriguez-Reinoso, F., Rouquerol, J., and Sing, K. S. (2015). Physisorption of gases, with special reference to the evaluation of surface area and pore size distribution (IUPAC Technical Report). *Pure and applied chemistry*, 87(9-10), 1051-1069.
- Wang, L., Shahbazi, A., and Hanna, M. A. (2011). Characterization of corn stover, distiller grains and cattle manure for thermochemical conversion. *Biomass and Bioenergy*, 35(1), 171–178.
- Wu, Z., Xie, J., Liu, H., Chen, T., Cheng, P., Wang, C., and Kong, D. (2018). Preparation, characterization, and performance of 4A zeolite based on opal waste rock for removal of ammonium ion. *Adsorption Science and Technology*, 36(9-10), 1700–1715.
- Yao, G., Lei, J., Zhang, X., Sun, Z., and Zheng, S. (2018). One-step hydrothermal synthesis of zeolite X powder from natural low-grade diatomite. *Materials*, 11(6), 906.

- Yu, C., Wang, H., Lu, M., Zhu, F., Yang, Y., Huang, H., Zou, C., Xiong, J., and Zhong, Z. (2020). Application of rice straw, corn cob, and lotus leaf as agricultural waste derived catalysts for low temperature SCR process: Optimization of preparation process, catalytic activity and characterization. *Aerosol and Air Quality Research*, 20(4), 862–876.
- Zhang, S., Cui, M., Chen, J., Ding, Z., Wang, X., Mu, Y., and Meng, C. (2019). Modification of synthetic zeolite X by thiourea and its adsorption for Cd (II). *Materials Letters*, 236, 233–235.
- Zulkifli, N. S. C., Ab Rahman, I., Mohamad, D., and Husein, A. (2013). A green sol-gel route for the synthesis of structurally controlled silica particles from rice husk for dental composite filler. *Ceramics International*, 39(4), 4559–4567.